TECHNICAL AND SCIENTIFIC VERIFICATIONS OF THE EUMETSAT MTG-FCI AMV PROTOTYPE

Manuel Carranza [1], Régis Borde [2]

[1] GMV Aerospace and Defence S.A. at EUMETSAT, Eumetsat Allee 1, D-64295 Darmstadt, Germany
[2] EUMETSAT, Eumetsat Allee 1, D-64295 Darmstadt, Germany

Abstract

In preparation for the launch of the first MTG-I satellite, currently scheduled for the fourth quarter of 2021, the MTG-FCI AMV prototype has been developed at EUMETSAT based on the current operational MSG AMV processor. In the framework of MTG's Ground Segment preparation, technical and scientific verifications of the MTG-FCI AMV prototype are currently ongoing using both MSG and Himawari-8 data.

A thorough comparison of the MSG and MTG AMV extraction algorithms has been performed using one month of MSG data (14th May to 14th June 2016) in order to test the impact of the main algorithm changes proposed for MTG-FCI (use of three images instead of four, no intermediate product averaging, etc.). The performances of the two schemes against forecast fields are presented in this paper.

DATA PREPARATION

The MTG-FCI AMV prototype developed at EUMETSAT is largely based on the operational MSG AMV extraction algorithm (Borde et al., 2014), with the following main differences:

- three images (at HH:15, HH:30 and HH:45) instead of four (at HH:00, HH:15, HH:30 and HH:45);
- reference image at HH:30 (with backward and forward tracking) instead of HH:00 (only forward tracking);
- no intermediate product averaging, the second intermediate component being used as final product instead;
- final AMV coordinates set to the position of the tracked feature, instead of the target centre (this was actually not considered in the present study, but it will be in the future)

In this study a series of comparisons are performed considering Atmospheric Motion Vectors (AMVs) extracted from the VIS0.8, WV6.2, WV7.3 and IR10.8 channels over the full MSG disk using one month of MSG data (14th May to 14th June 2016). Four configurations of the Meteosat Third Generation (MTG) Flexible Combined Imager (FCI) algorithm have been considered for the IR10.8 channel, using 12x12, 16x16, 20x20 and 24x24 target boxes to extract the AMVs, respectively; for the Meteosat Second Generation (MSG) algorithm, two configurations have been considered: 12x12 and 24x24 target boxes. For all other channels only a target-box size of 24x24 pixels has been considered. The Optimal Cloud Analysis (OCA) product has been used to set the AMV altitude in all cases.

In order to avoid any reference to the forecast model in the AMV extraction, the background wind guess has not been used to initiate the tracking of the AMVs. The limitation of the use of the model reference for AMV processing is a normal working practice at EUMETSAT.

The performance results are split by geographical area (global, northern hemisphere, southern hemisphere and tropics), as well as by altitude level (all, high, mid and low).

RESULTS

Processing time

The processing time is a critical parameter in an operational framework because all products have to be extracted within a limited amount of time. Table 1 summarizes the processing times needed to extract AMVs using the MSG and MTG algorithms for various target size boxes for the IR10.8 channel. The values correspond to the time to process one day in the first column, and to process one hour in the second column.

	Time per hour/final product	Time per processed day
MSG_24	2:48 min	1:07:23 hours
MTG-FCI_24	1:54 min	0:45:46 hours
MTG-FCI_20	1:59 min	0:47:40 hours
MTG-FCI_16	1:37 min	0:38:50 hours
MTG-FCI_12	1:42 min	0:40:45 hours

Table 1: Processing times for the nominal MSG algorithm and for MTG-FCI configurations that use 24x24, 20x20, 16x16 and 12x12 target boxes sizes, respectively, for the IR10.8 channel.

The MTG algorithm needs significantly less time to run than the MSG algorithm, regardless of the target-box size. According to these results, the optimal target-box size, considering only the computing time, seems to be 16x16, which is currently the nominal target-box size planned for MTG. Similar results were obtained using other channels, not shown here for simplicity.

AMV production

Table 2 shows the average number of AMVs per height level with quality index (QI) larger than 80 % extracted with the MSG and MTG algorithms using 24x24 pixel target boxes. From top left to bottom right, the tables correspond to AMVs extracted from channels VIS0.8, WV6.2, WV7.3 and IR10.8, respectively. The last column in each table shows the difference in the AMV production (in percentage, %) between the MTG-FCI and MSG algorithms.

	VIS 0.8 µm		
	MSG 24	MTG 24	MTG – MSG
all	3,426	3,832	+11.9%
high	830	829	–0.1%
mid	596	713	+19.6%
low	2,000	2,290	+14.6%

	WV 6.2 µm (cloudy)		
	MSG 24	MTG 24	MTG – MSG
all	4,057	4,077	+0.5%
high	3,897	3,858	–1.0%
mid	160	219	+37.7%
low	–	–	–

	WV 7.3 µm (cloudy)		
	MSG 24	MTG 24	MTG – MSG
all	5,175	5,138	–0.7%
high	4,091	4,028	–1.5%
mid	1,084	1,110	+2.5%
low	–	–	–

	IR 10.8 µm		
	MSG 24	MTG 24	MTG – MSG
all	7,614	8,231	+8.1%
high	3,358	3,317	–1.2%
mid	1,199	1,363	+13.7%
low	3,057	3,551	+16.2%

Table 2: Average number of AMVs extracted with the MSG and MTG algorithms (QI > 80).

Around 12 % and 8% more AMVs are extracted using the MTG-FCI algorithm with respect to the MSG algorithm from the VIS0.8 and IR10.8 channels, respectively. For both VIS0.8 and IR10.8 channels the increase in the AMV production occurs essentially at low and mid levels. The AMV production using

the WV channels is very similar for both algorithms.

AMV distribution

Figure 1 shows the geographical distribution of AMVs with QI larger than 80 extracted with the MSG and MTG-FCI algorithms, for the IR10.8 channel. The colour scale represents pressures in hPa. Other channels are not shown here for simplicity.

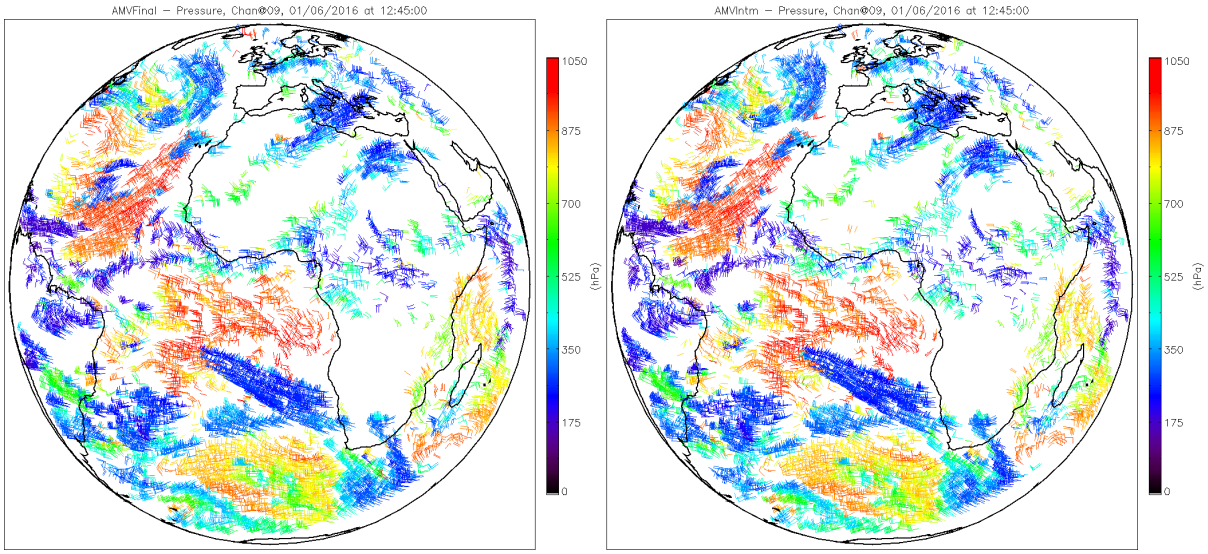

Figure 1: AMV distribution for the MSG (left) and MTG-FCI (right) algorithms on 01/06/2016 at 12:45 (IR10.8 channel).

The AMV distribution is fairly similar for both algorithms for all channels. There are some noticeable differences in some places, but overall the speed, direction and height of the AMVs are consistent between the two algorithms. For channels VIS0.8 and IR10.8 a slightly larger amount of AMVs can be appreciated for MTG-FCI with respect to MSG in certain areas, which is in agreement with the figures in Table 2.

AMV histograms

Figures 2 and 3 show the average AMV speed, direction and pressure histograms of VIS0.8 (left) and IR10.8 (right) AMVs extracted with the nominal MSG algorithm and the MTG-FCI algorithms.

For the IR10.8 channel, different target-box sizes have been considered using the MTG-FCI algorithm. The histograms are normalized by the total amount of AMVs, which means that the differences in the AMV production at mid and low levels are not captured in the plots.

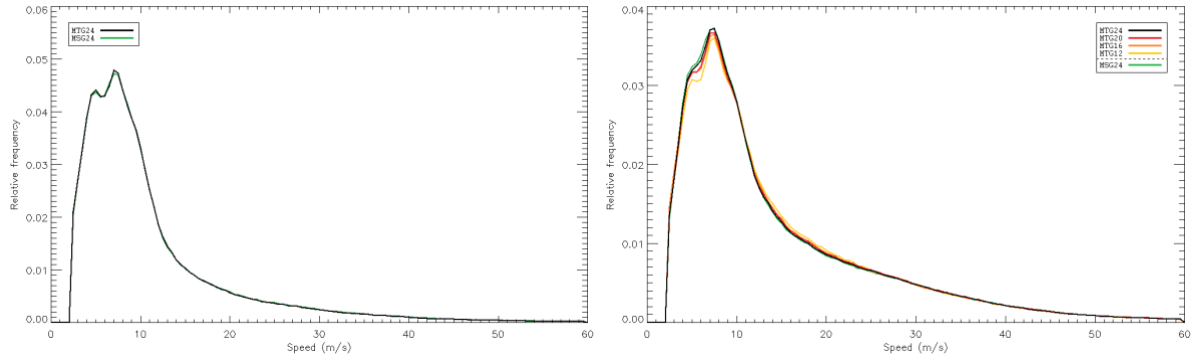

Figure 2: Average AMV speed histograms for AMVs extracted with the MSG (green) and MTG-FCI (black) algorithms using the VIS0.8 (left) and IR10.8 (right) channels.

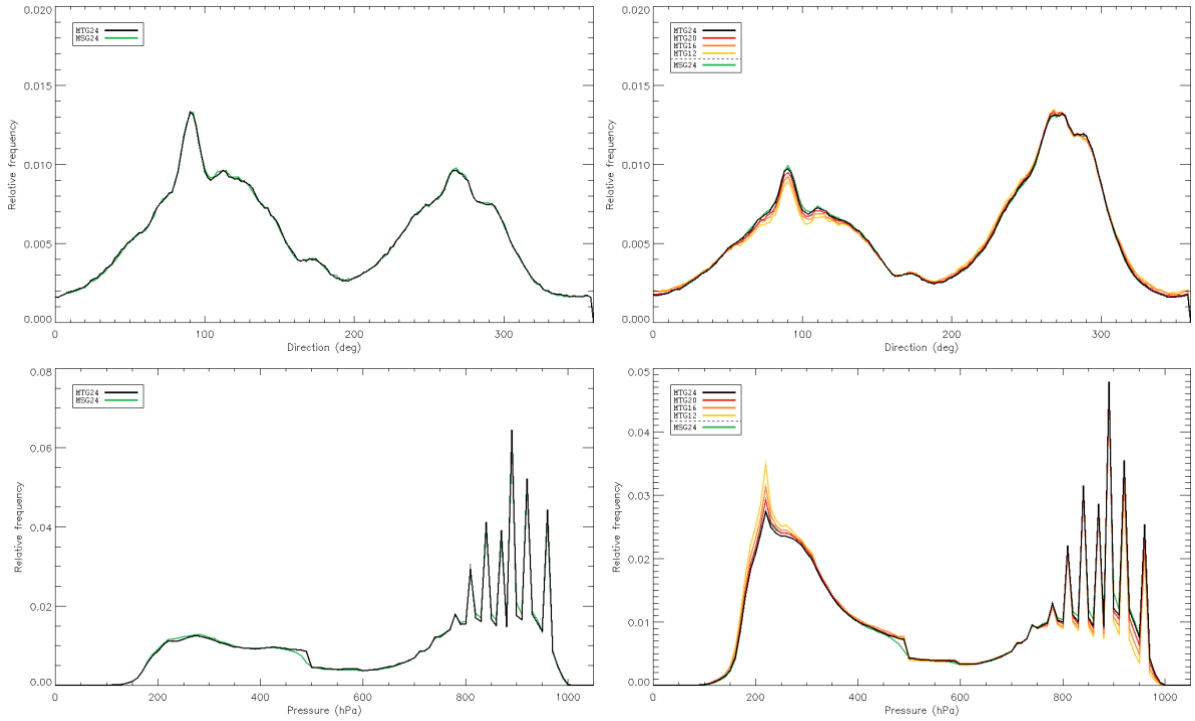

Figure 3: Average AMV direction (above) and pressure (below) histograms for AMVs extracted with the MSG (green) and MTG-FCI (black) algorithms using the VIS0.8 (left) and IR10.8 (right) channels.

AMVs extracted using the MSG algorithm are found a bit faster on average because there is a larger proportion of AMVs set at high levels than with the MTG-FCI algorithm. The differences regarding the AMV directions are negligible. The high-pressure peaks in the histograms are linked to the presence of low-level temperature inversion areas within the MSG processing disk; in such areas the altitude of the AMV is set to the level of the temperature inversion. The histograms of MSG and MTG-FCI AMVs are almost identical for the two water vapour channels, WV6.2 and WV7.3, both for cloudy and clear-sky AMVs (not shown here).

MSG vs MTG-FCI collocated AMVs

Figure 4 shows the average speed and pressure difference histograms of collocated AMVs, MSG minus MTG-FCI, for the considered channels: VIS0.8 (green), WV6.2 cloudy (light blue), WV6.2 clear-sky (light orange), WV7.3 cloudy (dark blue), WV7.3 clear-sky (dark orange) and IR10.8 (black). The AMVs have been collocated within boxes of 0.25 deg in both latitude and longitude, considering only speed values larger than 2.5 m/s and QI values larger than 80% for both MSG and MTG AMVs.

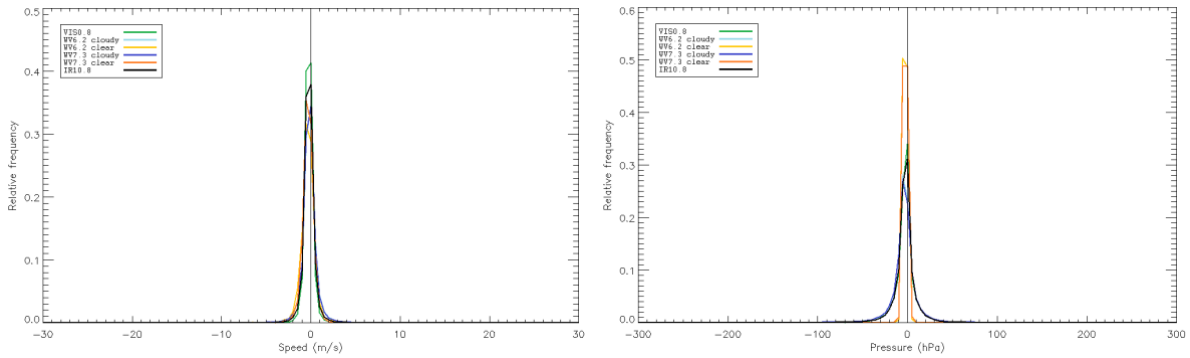

Figure 4: Average speed (left) and pressure (right) difference histograms of collocated AMVs using the VIS0.8 (green), WV6.2 cloudy (light blue), WV6.2 clear-sky (light orange), WV7.3 cloudy (dark blue), WV7.3 clear-sky (dark orange) and IR10.8 (black) channel.

The differences are very small in all cases, with the histograms clearly centred on the vertical axis. The same can be observed for the direction difference histograms (not shown here). In particular, for the speed histogram the mean is close to 0 m/s and the standard deviation is smaller than 1 m/s in all cases; for the direction histogram the mean is close to 0 deg in all cases, and the standard deviation ranges from 3 to 6 deg; and for the pressure histogram the mean is smaller than 1 hPa in absolute value in all cases, and the standard deviation ranges from 1 to 18 hPa. All this denotes a striking agreement between the results obtained with both algorithms.

Figure 5 shows speed, direction and pressure scatter plots of collocated AMVs extracted with the two algorithms for the IR10.8 channel. The agreement is very good for all variables, with a correlation coefficient close to 1 in all cases. This is in accordance with the histograms shown in Figures 3 and 4. It is a strong indication that both algorithms are able to track essentially the same features in the processed images (which was expected, because the tracking mechanism is the same in both cases).

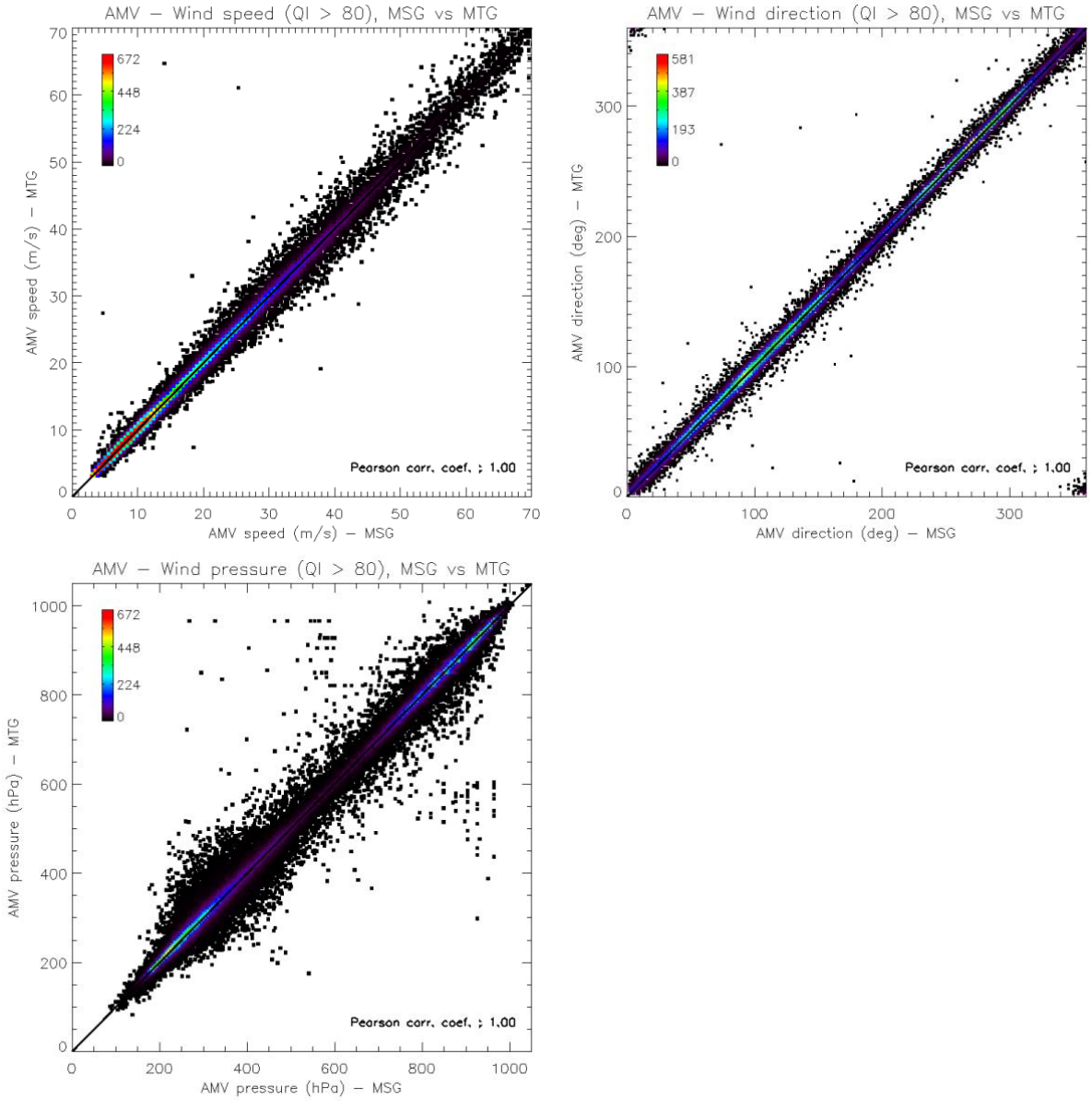

Figure 5: Speed (upper left), direction (upper right) and pressure (lower left) scatter plots of collocated AMVs extracted with the MSG and MTG-FCI algorithms using the IR10.8 channel.

Outliers and scattering are due to the collocation criteria, the use of 0.25x0.25 deg grid boxes, the averaging performed within the MSG scheme, and the fact that the MSG and MTG-FCI schemes use a different reference image (HH:00 for MSG, HH:30 for MTG-FCI) in this study. Indeed, this last point can lead to tracking different features, especially in the case of fast-moving clouds. The differences are much smaller when comparing corresponding MSG and MTG-FCI AMV intermediate products at the same time (not shown here).

Similar scatter plots were obtained for all other channels (VIS0.8, WV6.2 and WV7.3), but are not shown here for simplicity.

Statistics against forecast

The quality of the AMVs is usually assessed calculating the speed biases and Normalized Root Mean Square (NRMS) errors against collocated forecast fields or radiosonde observations following CGMS criteria defined at the Third International Winds Workshop (Menzel, 1996): horizontal distance smaller than 150 km, and vertical distance smaller than 25 hPa. Statistics against forecast fields are presented for cloudy AMVs extracted with the MSG and MTG-FCI algorithms using 24x24 target boxes. Tables 3 through 6 show the statistics for channels VIS0.8, WV6.2, WV7.3 and IR10.8 respectively. The results are split by geographical area and altitude level.

In the following tables, positive speed bias are shown in green, and negative speed bias in red. A green background represents an improvement for MTG with respect to the MSG algorithm (decrease in absolute value larger than 0.1 m/s for the speed bias, 0.05 m/s for the NRMS); a yellow background represents a neutral impact (difference in absolute value not larger than 0.1 m/s for the speed bias, 0.05 m/s for the NRMS); and a red background represents a degradation (increase in absolute value larger than 0.1 m/s for the speed bias, 0.05 m/s for the NRMS).

The MTG-FCI algorithms yields in general slightly smaller speed bias values than the MSG algorithm for all channels, geographical areas and levels, with some exceptions. For channel VIS0.8 the impact is slightly negative, especially in the southern hemisphere; but the MTG algorithm produces nearly 12% more AMVs (see Table 2). For channel IR10.8 the impact is fairly neutral, with largest differences for mid-level and low-level AMVs. For channels WV6.2 and WV7.3 there is a significant global improvement. However, there is as a slight degradation for AMVs in the southern hemisphere, particularly notorious for channel WV7.3.

The differences in NRMS values are negligible for all channels, geographical areas and levels.

	Speed bias – MSG 24			
	GLO	NH	TR	SH
all	–0.39	–1.05	0.26	–1.27
high	–1.42	–1.98	–0.35	–2.77
mid	–0.86	–1.30	0.15	–2.43
low	0.17	–0.24	0.48	–0.33

	Speed bias – MTG 24			
	GLO	NH	TR	SH
all	–0.53	–1.20	0.19	–1.47
high	–1.45	–2.02	–0.39	–2.81
mid	–0.87	–1.28	0.15	–2.55
low	0.09	–0.35	0.46	–0.48

	NRMS – MSG 24			
	GLO	NH	TR	SH
all	0.30	0.28	0.34	0.25
high	0.27	0.25	0.35	0.21
mid	0.35	0.32	0.44	0.28
low	0.24	0.24	0.26	0.19

	NRMS – MTG 24			
	GLO	NH	TR	SH
all	0.31	0.29	0.36	0.25
high	0.28	0.26	0.36	0.22
mid	0.37	0.33	0.46	0.30
low	0.25	0.25	0.28	0.19

Table 3: Speed bias and NRMS for the MSG (left) and MTG-FCI (right) algorithms using the VIS0.8 channel.

	Speed bias – MSG 24			
	GLO	NH	TR	SH
all	1.00	0.80	1.59	0.23
high	0.91	0.62	1.53	0.09
mid	3.21	3.61	5.24	2.24
low	–	–	–	–

	Speed bias – MTG 24			
	GLO	NH	TR	SH
all	0.91	0.70	1.58	0.19
high	0.78	0.40	1.54	–0.04
mid	3.21	3.85	3.56	2.68
low	–	–	–	–

	NRMS – MSG 24			
	GLO	NH	TR	SH
all	0.24	0.22	0.32	0.18
high	0.23	0.21	0.32	0.17
mid	0.34	0.36	0.61	0.27
low	–	–	–	–

	NRMS – MTG 24			
	GLO	NH	TR	SH
all	0.24	0.23	0.39	0.17
high	0.23	0.22	0.38	0.17
mid	0.33	0.39	0.62	0.27
low	–	–	–	–

Table 4: Same as Table 3 for the WV6.2 channel (cloudy AMVs).

	Speed bias – MSG 24			
	GLO	NH	TR	SH
all	0.31	0.31	1.04	–0.76
high	0.15	–0.12	1.01	–1.06
mid	1.10	1.98	1.26	0.34
low	–	–	–	–

	Speed bias – MTG 24			
	GLO	NH	TR	SH
all	0.13	0.11	1.01	–0.92
high	–0.02	–0.40	1.05	–1.21
mid	0.82	1.81	0.70	0.17
low	–	–	–	–

	NRMS – MSG 24			
	GLO	NH	TR	SH
all	0.25	0.24	0.34	0.20
high	0.23	0.21	0.32	0.18
mid	0.35	0.37	0.55	0.28
low	–	–	–	–

	NRMS – MTG 24			
	GLO	NH	TR	SH
all	0.26	0.25	0.40	0.19
high	0.24	0.22	0.38	0.18
mid	0.35	0.38	0.54	0.28
low	–	–	–	–

Table 5: Same as Table 3 for the WV7.3 channel (cloudy AMVs).

	Speed bias – MSG 24			
	GLO	NH	TR	SH
all	–0.33	–0.57	0.48	–1.51
high	–0.64	–0.96	0.57	–2.30
mid	–0.50	–0.21	0.59	–2.01
low	0.11	0.00	0.36	–0.35

	Speed bias – MTG 24			
	GLO	NH	TR	SH
all	–0.39	–0.61	0.51	–1.62
high	–0.64	–0.97	0.57	–2.29
mid	–0.31	0.00	0.77	–1.85
low	0.00	–0.10	0.34	–0.53

	NRMS – MSG 24			
	GLO	NH	TR	SH
all	0.27	0.26	0.34	0.23
high	0.25	0.23	0.32	0.20
mid	0.34	0.33	0.47	0.28
low	0.24	0.30	0.25	0.20

	NRMS – MTG 24			
	GLO	NH	TR	SH
all	0.28	0.26	0.35	0.23
high	0.25	0.23	0.32	0.20
mid	0.35	0.34	0.49	0.29
low	0.24	0.32	0.27	0.19

Table 6: Same as Table 3 for the IR10.8 channel.

Impact of the target-box size

AMVs have been assimilated in NWP global models for a long time. The recent evolution towards regional models needs assimilation of smaller scale observations to improve the forecast. Several ways have been investigated to try to extract smaller scale wind information by using rapid scan imagery or smaller tracer sizes. Garcia-Pereda and Borde (2014) have studied the impact of the target-box size on the extraction of AMVs from the MSG SEVIRI instrument. They have shown that the larger the tracer size, the easier the matching because large target boxes contain generally good contrast and entropy to select a good tracer in the first image and to follow it in the later images. But the tracer size is also linked to the size and lifetime of the selected feature. The search of an optimized configuration to be used operationally is not easy, and it implies to find a balance between different impacts like the number of good AMVs extracted, the accuracy of the tracking or the performance against other reference winds.

Figure 6 shows the speed bias of AMVs extracted by the MSG (blue colour) and the MTG-FCI (red colour) algorithm using various target-box sizes. Only AMVs extracted from the IR10.8 channel and with QI above 80% have been considered. Two configurations of the MSG algorithm, MSG 12 and MSG 24, and four configurations of the MTG-FCI algorithm, MTG 12, MTG 16, MTG 20 and MTG 24, have been tested. The groups of bars represent from left to right the results for all AMVs, high-level AMVs, mid-level AMVs and low-level AMVs, respectively.

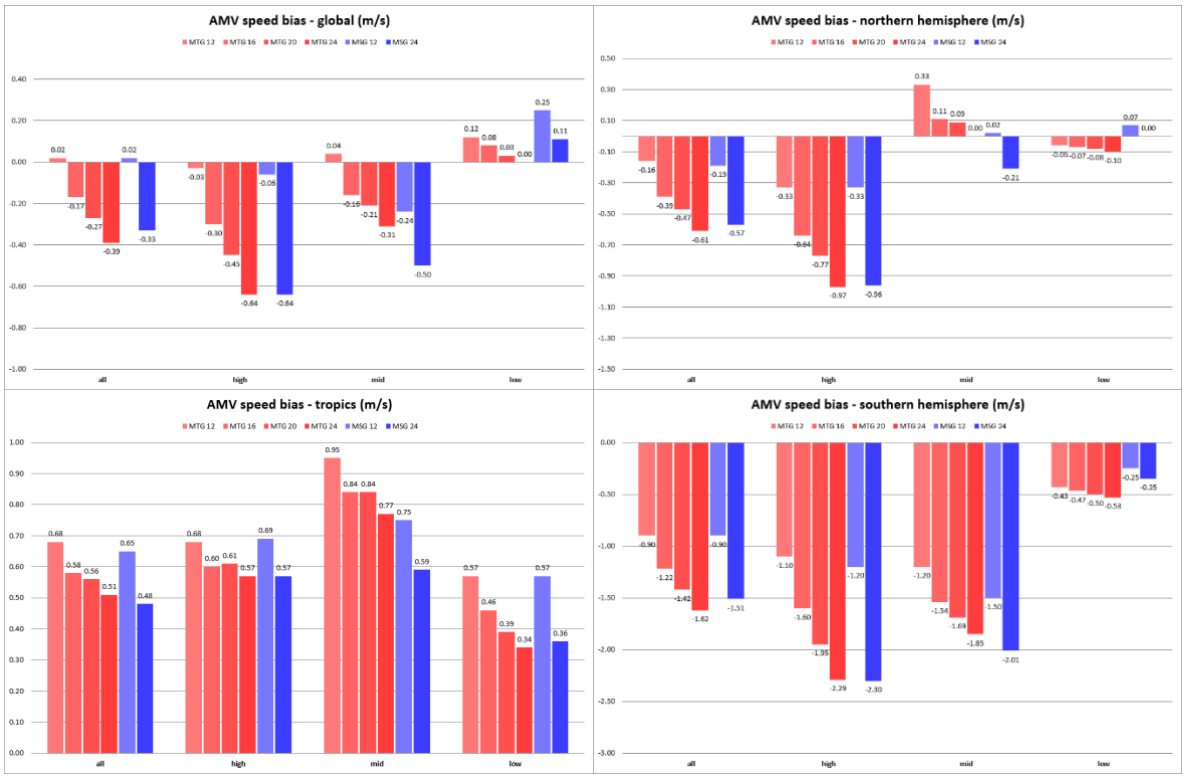

Figure 6: Channel IR10.8 AMV speed bias against forecast for the MSG (blue) and MTG (red) algorithms, global (top left), northern hemisphere (top right), tropics (bottom left) and southern hemisphere (bottom right).

In general the speed bias decreases when the target box size increases, in accordance with the common observation that smaller target boxes yield faster AMVs (Bresky et al, 2012; García-Pereda and Borde, 2014). The global average speed bias is in general negative, except at low levels, which is in agreement with previous observations and analyses performed at EUMETSAT. Geographically, the average speed bias is mostly negative in the northern hemisphere (except at mid levels), positive in the tropics, and negative in the southern hemisphere.

Figure 7 shows the global average AMV speed NRMS against forecast for the MSG and MTG-FCI

algorithms for the 10.8 µm channel, separated by height level (only AMVs with QI above 80%). The NRMS values are very similar for both schemes and all levels.

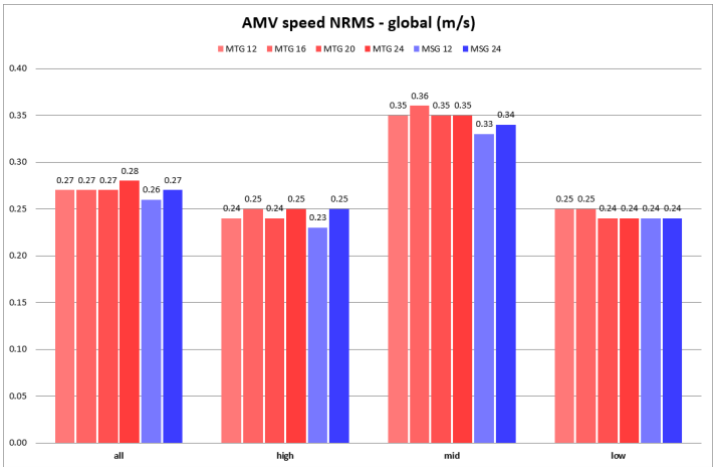

Figure 7: Channel IR10.8 global AMV speed NRMS against forecast for the MSG (blue) and MTG (red) algorithms.

CONCLUSIONS

The performance of the MSG and MTG AMV algorithms has been analysed using one month of MSG data (14th May to 14th June 2016). The MSG algorithm produces fewer AMVs as a consequence of the intermediate product averaging process used, especially noticeable for the VIS0.8 and IR10.8 channels.

The AMV speed, direction and pressure histograms are very similar for both schemes, with slightly faster and higher AMVs for MSG on average. The main reason for this is the larger number of low-level and mid-level AMVs obtained using the MTG algorithm, which results in a smaller average speed. As illustrated by the AMV speed, direction and pressure scatter plots, as well as the difference histograms, the differences between the MTG final products and the corresponding MSG intermediate products are negligible.

The AMV speed statistics against forecast are very similar for both schemes, with slightly smaller values for the MTG-FCI algorithm on average. In general the speed bias decreases when the target box size increases, in accordance with previous observations and studies. The differences in the speed NRMS are very small.

The use of four images and the averaging process implemented within the MSG algorithm do not show a significant positive impact in comparison with the MTG-FCI scheme. The results shown in this study validate the strategy planed for the operational MTG-FCI AMV processor. The AMV final product will be based on the second intermediate component, providing a more instantaneous information on the wind field. Besides, the MTG-FCI AMV algorithm will be more similar to the schemes already used for the AVHRR instrument at EUMETSAT, and by other agencies.

Due to the similar spectral and spatial characteristics with respect to AHI (Advanced Himawari Imager), the scientific validation of the MTG-FCI AMV processor will be assessed using Himawari-8 data. Thanks to collaborations with the Japan Meteorological Agency (JMA) and the Korea Meteorological Administration (KMA), the MTG-FCI AMV prototype has been successfully adapted to use Himawari-8 data, and AMVs extracted with the MTG-FCI prototype will be compared against those extracted with the Himawari and GeoKompsat AMV algorithms.

REFERENCES

Borde, R., M. Doutriaux-Boucher, G. Dew and M. Carranza (2014): “A direct link between feature tracking and height assignment of operational EUMETSAT atmospheric motion vectors”. J. Atmos. Oceanic Technol., 31, 33–46.

Bresky, W., J. Daniels, A. Bailey and S. Wanzong (2012): “New methods toward minimizing the slow speed bias associated with atmospheric motion vectors”. J. Appl. Meteor. Climatol., 51, 2137-2151.

Carranza, M., R. Borde and M. Doutriaux-Boucher (2014): “Recent changes in the derivation of geostationary atmospheric motion vectors at EUMETSAT”. Proceedings of the Twelfth International Winds Workshop, Copenhagen, Denmark.

García-Pereda, J. and Borde R. (2014): “The impact of the tracer size and the temporal gap between images in the extraction of atmospheric motion vectors”. J. Atmos. Oceanic Technol., 31, 1761–1770.

Menzel, W.P. (1996): “Report on the Working Group on verification statistics”. Proceedings of the Third International Winds Workshop, Ascona, Switzerland.